Int. J. Solids Structures Vol. 30, No. 6, pp. 835–856, 1993
Printed in Great Britain

0020–7683/93 $6.00+ .00

ANALYSIS OF PLASTIC BUCKLING OF STEEL PLATES

TETSURO INOUE
Institute of Engineering Mechanics, University of Tsukuba, Tsukuba, Japan

and

BEN KATO
Department of Architecture, University of Toyo, Kawagoe, Japan

(*Received* 26 *September* 1991 ; *in revised form* 17 *August* 1992)

Abstract—Plasticity in steel is characterized by an appreciable amount of plastic flow (in the yield plateau range) which precedes strain hardening. This study is devoted to an analytical evaluation of the effective plastic shear modulus of fully yielded steel plates at the instant of buckling. It is assumed that yielding of steel is to follow the Tresca yield criterion and that plastic deformation of a steel plate is to be caused by slips. The Tresca yield criterion provides lower bending stiffnesses than that obtained from the von Mises yield criterion, but it does not lower the plastic shear modulus of the material at any point on the yield plateau. A new theory is proposed here that assumes a nonuniform distribution of slips depending on the orientation of an infinite number of possible slip planes at each point in the plate. The twisting of the plate is then accompanied by distortion of its sectional shape, and this mode of buckling is shown to provide a considerable reduction in the effective plastic shear modulus. Applying these sectional stiffnesses and solving a differential equilibrium equation leads to a lower bifurcation strength, which provides much better correlations with experimental results than previous predictions.

1. INTRODUCTION

Analysis of plastic buckling of plates has a long historical background. The earliest such analysis is based on deformation theory, which is even now considered to give good correlation with experimental results. However these theories are not rational in the event of nonproportional loading, such as that which occurs in plate buckling. After deformation theory, incremental theory was proposed, which seemed to be rational, but was found to provide unacceptably higher plastic buckling bifurcation stresses of plates than experimental results. This is attributed to the assumption of a smooth yield surface, such as that associated with the von Mises yield criterion. Recently, from the viewpoint that the yield surface may have corners, plasticity rules have been reconsidered in order to justify the deformation theory.

All of the above-mentioned theories, however, deal with metals with round-house type stress–strain curves whenever yield flow does not occur. Since the plastic behavior of materials is most pronounced in the material with yield flow, such theories should also be able to explain test results for materials with an apparent yield flow such as mild steel. Unfortunately, all of the theories trying to justify the deformation theory assume that the yield surface maintains its original shape in the plastic flow range. Thus, the shear modulus in the plastic flow range is equal to the elastic shear modulus. Therefore, these theories cannot explain the plastic buckling of mild steel, and deformation theory is not applicable to materials with a plastic flow.

In order to overcome these difficulties, a completely different approach is developed here. It is based on the idea that the effective plastic shear modulus may be significantly reduced from the elastic value. Cruciform-section columns under compression, which are often used to study torsional buckling of plates, are employed in order to investigate the buckling of mild steel, from which rationally lower bifurcation stresses will be obtained for the plate element constituting the section.

Attention is focused on only one of the four plates in a cruciform-section column which is subjected to uniaxial compression and is under the boundary condition that three of its edges are simply supported, while another edge is free. The constituent material is mild

steel which has a clear yield point and an appreciable amount of plastic flow before subsequent strain hardening. In the yield plateau range, mild steel is strained under an almost constant stress. From this fact, it is assumed that a constant yield stress holds and therefore the longitudinal tangent modulus becomes zero in this range. The width-to-thickness ratio of the plate is small enough that elastic buckling does not take place. The bifurcation stress of the plate is then derived from solving a differential equation governing equilibrium which includes explicitly the bending and torsional stiffnesses. Since, in the yield plateau range, the sectional stiffnesses do not all vanish, it follows that a plate with a sufficiently small width-to-thickness ratio can be compressed stably into the yield plateau or even into the strain hardening range.

A number of studies have been devoted to the plastic buckling of plates. Using his famous column model, Shanley (1947) first demonstrated that the bifurcation point of a centrally compressed short column coincides theoretically with the tangent modulus load. This is known as Shanley's tangent modulus theory. Hill (1958) later generalized Shanley's concept and established a uniqueness criterion for the mathematical solution of elastic–plastic solids. This concept is now universally accepted in succeeding research work.

As mentioned before, deformation theory and incremental theory predict different values for the plastic bifurcation stress. In order to reduce the gap between the two predictions, the following treatments incorporating imperfections have been proposed: Onat and Drucker (1953) showed that the maximum load derived from incremental theory is reduced to the bifurcation load derived from deformation theory by considering unavoidably small imperfections in a cruciform-section column composed of a material with a bilinear stress–strain relation. Later, Hutchinson and Budiansky (1976) examined the imperfection-sensitivity associated with the incremental theory in a more generalized setting, again using a cruciform-section column. Their material had the mechanical properties represented by the Ramberg–Osgood relation, and their study contains the research scope of Onat and Drucker (1953) as a special case.

Some important proposals have attempted to reconcile the discrepancy between deformation theory and incremental theory for strain-hardening materials without considering imperfection. Batdorf and Budiansky (1949) proposed a slip theory of plasticity. Using this theory Batdorf (1949) studied the plastic buckling of a long flange plate and found that the plastic shear modulus is almost equivalent to that derived from the deformation theory. Budiansky (1959) later theoretically proved that, under any loading close to proportional loading, the slip theory is equivalent to the deformation theory.

Sewell (1973) solved for the bifurcation stress of a uniaxially compressed plate whose periphery is simply supported. He studied the effect of coupled hardening between the yield surface facets which meet at a vertex where the yield surface is locally similar to that of Tresca. He obtained bifurcation stresses that are 10–30% lower than those based on the von Mises yield criterion. This reduction is due to the reduction in the bending stiffnesses and is not due to the reduction in the plastic shear modulus. In fact, no reduction in shear modulus is obtained from his theory. Without a drastic reduction in the shear modulus, the results of bifurcation analysis will not be consistent with those of experiment. Sewell (1974) later proposed a general plastic flow theory for a multiple yield system in which the yield surface is assumed to be a pyramidal vertex of the type introduced by Hill (1966). He found that his theory generalizes and refines Budiansky's study, and that therefore it too is almost equivalent to the deformation theory for special loading conditions. Christoffersen and Hutchinson (1979) proposed J_2 corner theory, which can be regarded as an extension of Budiansky's (1959) theory, to reassess the deformation theory. They concretely applied the theory to the bifurcation and imperfection-sensitivity analysis of necking in a thin sheet.

Buckling analysis of plates using the deformation theory is continued by Ore and Durban (1989). However, since they deal with a material whose mechanical properties are defined by a Ramberg–Osgood relation without a yield flow, their research may be classified into the group trying to justify the deformation theory.

The investigations into the plastic buckling of plates described above have considered the possible stress versus strain relationships only based on the plasticity theory from rather microscopic viewpoints. In contrast, the approach presented here focuses on stress versus

strain relationships at the bifurcation point that are derived from a less restricted mode of buckling deformation and from a more macroscopic viewpoint which may be described as follows: Yielding is taken to follow the Tresca yield criterion. Plastic deformation of the plate is caused by slips which develop only in the directions of maximum shear stress. Assuming a nonuniform distribution of slips, the plate is capable of twist accompanied by distortion of its cross-sectional shape. In the case of torsional buckling, this mode of buckling provides a much lower sectional shear stiffness. In view of the particular plasticity theory used here, the component of buckling shear strain is not different from that obtained in the previous purely elastic studies. However, the effective plastic shear modulus is reduced significantly below the elastic value, because the rate of exerted elastic shear strain is much less.

The effective plastic shear modulus and bending stiffnesses are obtained individually because two modes of torsion and bending are assumed to take place by superposition at the instant of plate buckling. The derived shear modulus has an identical value both in the yield plateau and in the strain hardening range. All the bending stiffnesses vanish in the yield plateau range. One of them is again nonzero in the strain hardening range, but is small enough to neglect its contribution to any increase in the buckling strength. The derived bifurcation strengths provide much better correlations with experimental results than those given by previous predictions.

2. STRAIN COMPONENTS IN A YIELDED PLATE

Strain components in a yielded plate in the plastic flow range under the condition of uniaxial compression and plane stress are investigated in this chapter. Yielding is assumed to follow the Tresca yield criterion and the plastic deformation is generated by planar slipping in the direction of maximum shear stress. Under uniaxial compression, the plane of maximum shear stress coincides with the plane making an angle of $\pi/4$ with the direction of the axial stress. Therefore, any tangent plane to a cone with a vertical angle of $\pi/2$ can be the slip plane as shown in Fig. 1.

Now, one of the possible slip planes is represented by the tangent plane to the cone at line $O'S$ which is involved in the plane making an angle of k with the xy-plane in the fixed coordinate system shown in Fig. 1. A local coordinate system is defined such that point S is the origin, OS is the y'-axis, the tangent to the circle at point S is the z'-axis, and the line parallel to the x-axis and passing through point S is the x'-axis. This local coordinate system can be established by rotating the fixed coordinate system by a counterclockwise angle k about the x-axis. The $x'y'$ plane is normal to the slip plane, and the angle of inclination of the $y'z'$-plane to the slip plane is $\pi/4$. The components of plastic strain are analysed in this local coordinate system, when the axial stress is applied in the x direction. In Fig. 1, σ_0 represents the absolute yield stress and a minus sign is attached for compression.

The slip deformations in the tangent planes at $O'S$ and $O'S'$ lines involved in the $x'y'$-plane defined in Fig. 1 are illustrated in Fig. 2. Both slip deformations are not necessarily equal, but they are considered to be a pair corresponding to the principal strain in the same

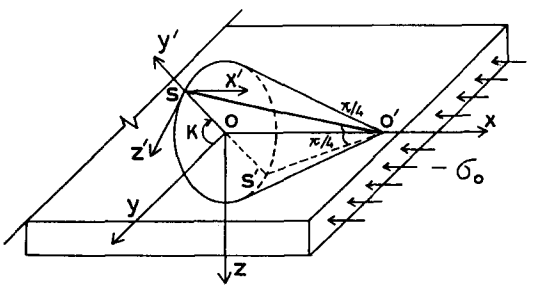

Fig. 1. Slip plane.

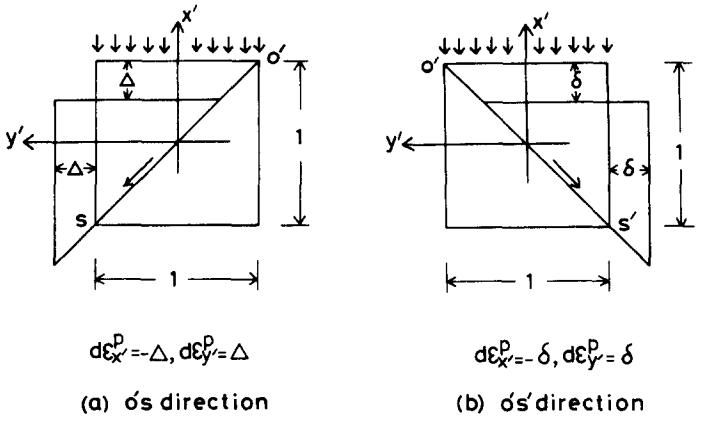

Fig. 2. Slip model.

direction. Since the axes of x', y' and z' are axes of principal strains, components of plastic strain are given by

$$d\varepsilon^p_{x'} = -\lambda, \quad d\varepsilon^p_{y'} = \lambda, \quad d\varepsilon^p_{z'} = 0, \tag{1}$$

where

$d\varepsilon^p_{x'}$ = increment of plastic principal strain in the x' direction,

$d\varepsilon^p_{y'}$ = increment of plastic principal strain in the y' direction,

$d\varepsilon^p_{z'}$ = increment of plastic principal strain in the z' direction,

λ = positive scalar representing the increment of plastic strain related to the sum of Δ and δ in Fig. 2.

It is noted that increments of plastic shear strains denoted by $d\gamma^p_{x'y'}$, $d\gamma^p_{y'z'}$, and $d\gamma^p_{z'x'}$, are equal to zero.

The strain components defined by eqns (1) can be transformed to those in the fixed coordinate system. The component in the x direction is the same as that in the x' direction. The components in the y and z directions are determined from the well-known transformation rule. The transformation of principal strains into the coordinate system making a clockwise angle of Ω with the axis of maximum principal strain is represented by

$$\varepsilon_n = \frac{\varepsilon_1+\varepsilon_2}{2} + \frac{\varepsilon_1-\varepsilon_2}{2}\cos 2\Omega, \quad \frac{\gamma}{2} = -\frac{\varepsilon_1-\varepsilon_2}{2}\sin 2\Omega, \tag{2}$$

where

ε_1 = λ, larger principal strain (y' direction),

ε_2 = 0, smaller principal strain (z' direction),

ε_n = normal strain in the direction making a clockwise angle of Ω with the direction of the maximum principal strain,

γ = shear strain after transformation.

Substituting $\varepsilon_1 = \lambda$, $\varepsilon_2 = 0$ and $\Omega = k$ into the first equation in eqns (2), the increment of plastic normal strain in the y direction is obtained. Substituting $\varepsilon_1 = \lambda$, $\varepsilon_2 = 0$ and $\Omega = k+\pi/2$ into the first equation in eqns (2), the increment of plastic normal strain in the z direction is obtained. Substituting $\varepsilon_1 = \lambda$, $\varepsilon_2 = 0$ and $\Omega = k$ into the second equation in eqns (2), the increment of plastic shear strain in the yz-plane is obtained. The shear strains in the xy- and xz-planes all vanish. Therefore, the increments of plastic strains in the fixed coordinate system are represented by

$$d\varepsilon_x^p = -\lambda, \quad d\varepsilon_y^p = \lambda\cos^2 k, \quad d\varepsilon_z^p = \lambda\sin^2 k,$$
$$d\gamma_{xy}^p = 0, \quad d\gamma_{yz}^p = -\lambda\sin 2k, \quad d\gamma_{zx}^p = 0. \tag{3}$$

Equations (3) give the increments of plastic strains in the fixed coordinate system when slipping takes place in the planes defined by the angles of k and $k+\pi$. In general, deformation of a plate due to compression, tension, bending and torsion is generated by combined slipping in various slip planes. For example, when a stable yield slip takes place due to the axial force in the x direction as shown in Fig. 1, the increments of plastic strains in the tangent planes defined by $k = 0$ and $k = \pi$ are represented by $d\varepsilon_x^p = -\lambda$, $d\varepsilon_y^p = \lambda$ and $d\varepsilon_z^p = 0$; and the increments of plastic strains in the tangent planes defined by $k = \pi/2$ and $k = 3/2\pi$, represented by $d\varepsilon_x^p = -\lambda$, $d\varepsilon_y^p = 0$ and $d\varepsilon_z^p = \lambda$. These two families of slip are generated simultaneously. The following resultant increments are then obtained, which represent the incompressible and isotropic flow rule:

$$d\varepsilon_x^p = -2\lambda = -\mu, \quad d\varepsilon_y^p = \lambda = \frac{\mu}{2}, \quad d\varepsilon_z^p = \lambda = \frac{\mu}{2}. \tag{4}$$

3. STRAINS AND DEFORMATION IN A PLATE IN TORSION

Strains and deformation in a plate subjected to uniaxial compression at the instant of torsional buckling are investigated in this chapter on the condition that the full section is yielded in the yield plateau range. It is assumed that, at the instant of torsional buckling, the increments of plastic strains take place as described in the previous chapter. Axial strains and shear strain are generated simultaneously without any strain reversal in this model, which is similar to the Shanley model in that axial and flexural strains take place simultaneously at the instant of flexural buckling. Therefore, this model will give the minimum buckling load.

Figure 3 shows a plate in torsion under axial yield force. According to eqns (3), the increments of axial strains are accompanied by the increment of shear strain in the yz-plane except for the planes of $k = 0$ and $\pi/2$. Because the plate is in torsion, the following three conditions are assumed:

(1) At any point along the length, the rate of the torsional angle is constant.

(2) The increments of plastic normal strains $d\varepsilon_x^p$, $d\varepsilon_y^p$ and $d\varepsilon_z^p$ are constant over the length.

(3) The increment of plastic shear strain $d\gamma_{yz}^p$ is simple shear strain.

The combination of assumptions (1) and (3) requires that the value of $d\gamma_{yz}^p$ be proportional to the x-coordinate. Figure 3 is based on these assumptions, and this mode shows a progressive simple shear deformation accompanied by warp. Assumption (3), however, will be shown to follow as a necessary condition in Chapter 7 by considering the boundary conditions.

Assumptions (1) and (3) give

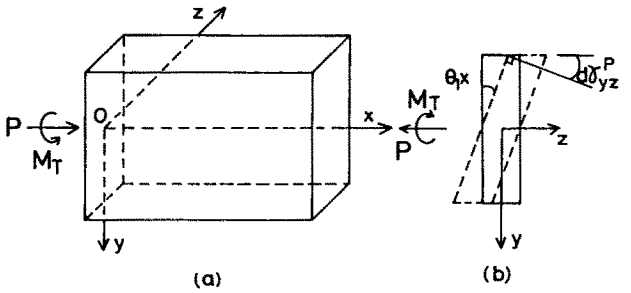

Fig. 3. Torsional deformation.

$$d\gamma_{yz}^{p} = -\theta_1 x = -\bar{x}\theta_l, \quad \bar{x} = x/l, \tag{5}$$

where

θ_1 = torsional angle per unit length,

l = length,

θ_l = torsional angle at the end ($x = l$).

From eqns (3) and (5),

$$\lambda \sin 2k = \bar{x}\theta_l. \tag{6}$$

Considering that the angle k of the slip plane at the end coincides with the direction in which the absolute value of $d\gamma_{yz}^{p}$ becomes maximum, the maximum absolute value of $d\gamma_{yz}^{p}$ is obtained from eqns (3) to be $-\lambda$ when $k = \pi/4$. The angle $k = \pi/4 + \pi$ also provides the same maximum value related to the other perpendicular slip plane. Substituting $k = \pi/4$ and $\bar{x} = 1$ into eqn (6), we obtain

$$\lambda = \theta_l. \tag{7}$$

From eqns (6) and (7), we obtain

$$k = \tfrac{1}{2}\sin^{-1}\bar{x} \quad (0 \leqslant k \leqslant \pi/4). \tag{8}$$

It is noticed from eqns (3) that the same value for $d\gamma_{yz}^{p}$ is generated at the angle $k' = \pi/2 - k$ as at the angle k, and thus that the slip planes at k and k' can be combined.

The second condition characterizing this deformation is satisfied when the amounts of slip in the planes defined by k and k' are equal. Therefore, from eqns (3), we obtain

$$d\varepsilon_y^{p} = \lambda[\tfrac{1}{2}\cos^2 k + \tfrac{1}{2}\cos^2 k'] = \tfrac{1}{2}\lambda\left[\cos^2 k + \cos^2\left(\frac{\pi}{2} - k\right)\right] = \tfrac{1}{2}\lambda.$$

From a similar calculation, we obtain

$$d\varepsilon_z^{p} = \tfrac{1}{2}\lambda, \quad d\varepsilon_x^{p} = -\lambda.$$

From these equations, it is noted that $d\varepsilon_x^{p}$, $d\varepsilon_y^{p}$ and $d\varepsilon_z^{p}$ are constant over the length. For the case of pure compressive yielding, as investigated in Chapter 2, shear slip takes place in the two slip planes ($k = 0$ and π) which are invariant over the length. For the present torsional case, however, shear slips take place in the complex slip planes defined by k and k' which vary along the length according to eqn (8).

4. SHEAR MODULUS

Torsional stiffness is investigated in this chapter on the basis of Saint-Venant's principle (1855) and Prandtl's membrane analogy (1906). However, unlike the Saint-Venant theory which assumes for elastic materials that no shear strain exists in the yz-plane and which also assumes that the sectional shape remains the same after applying torsion, here we assume that the yz-plane is subjected to a shear deformation under the plastic condition according to the results obtained in the previous chapters.

When simple shear strain $d\gamma_{yz}^{p}$ is generated as shown in Fig. 3(b), the displacements of the small element are represented by

$$u = -\theta_1 xy, \quad v = 0, \quad \bar{w} = \theta_1 \varphi(y, z), \tag{9}$$

where

u = displacement in the z direction,

v = displacement in the y direction,

$\bar{w}$ = warping of cross-section in the x direction.

From eqns (9), we obtain

$$\left.\begin{aligned} \mathrm{d}\gamma_{zx} &= \frac{\partial \bar{w}}{\partial z} + \frac{\partial u}{\partial x} = \theta_1\left(\frac{\partial \varphi}{\partial z} - y\right) \\ \mathrm{d}\gamma_{yx} &= \frac{\partial \bar{w}}{\partial y} + \frac{\partial v}{\partial x} = \theta_1 \frac{\partial \varphi}{\partial y} \\ \mathrm{d}\gamma_{yz} &= \frac{\partial v}{\partial z} + \frac{\partial u}{\partial y} = -\theta_1 x = \mathrm{d}\gamma_{yz}^{\mathrm{p}} \end{aligned}\right\}. \tag{10}$$

Since $\mathrm{d}\gamma_{zx}$ and $\mathrm{d}\gamma_{yx}$ in eqns (10) have only elastic components, the following stress–strain relations are applicable:

$$\left.\begin{aligned} \tau_{zx} &= G\theta_1\left(\frac{\partial \varphi}{\partial z} - y\right) \\ \tau_{yx} &= G\theta_1 \frac{\partial \varphi}{\partial y} \end{aligned}\right\}, \tag{11}$$

where

$G = (E/2(1+\nu))$ = elastic shear modulus,

$E = 2.059 \times 10^5\,\mathrm{N\,mm^{-2}}$ = Young's modulus,

$\nu = 0.3$ = Poisson's ratio,

τ_{zx}, τ_{yx} = shear stresses in the zx and yx components, respectively (note that τ_{zx} and τ_{yx} are increments).

Since the equilibrium condition of the small element is given by $\partial\sigma_x/\partial x = 0$, we obtain

$$\frac{\partial \tau_{zx}}{\partial z} + \frac{\partial \tau_{yx}}{\partial y} = 0. \tag{12}$$

Equation (12) is satisfied by the stress function $\Psi(y, z)$ defined by

$$\left.\begin{aligned} \tau_{zx} &= \frac{\partial \Psi}{\partial y} \\ \tau_{yx} &= -\frac{\partial \Psi}{\partial z} \end{aligned}\right\}. \tag{13}$$

From eqns (11) and (13), we obtain

$$\left.\begin{aligned}\frac{\partial \Psi}{\partial y} &= G\theta_1\left(\frac{\partial \varphi}{\partial z} - y\right)\\ \frac{\partial \Psi}{\partial z} &= -G\theta_1\frac{\partial \varphi}{\partial y}\end{aligned}\right\}. \tag{14}$$

The sum of the partial derivatives of the first and second equations of eqns (14) with respect to y and x, respectively, results in

$$\frac{\partial^2 \Psi}{\partial z^2} + \frac{\partial^2 \Psi}{\partial y^2} = -G\theta_1. \tag{15}$$

From the shear stresses in eqns (13), we obtain the following torsional moment M_T considering that Ψ is zero at the boundary:

$$M_T = 2\int\int_A \Psi \, dA. \tag{16}$$

Equation (15) is similar to the following Prandtl's equation representing the equilibrium equation of a weightless membrane with a closed boundary under air pressure:

$$\frac{\partial^2 \zeta}{\partial z^2} + \frac{\partial^2 \zeta}{\partial y^2} = -\frac{p}{T}, \tag{17}$$

where

ζ = displacement of the membrane ($\zeta = 0$ at the boundary),

p = pressure per unit area in the membrane,

T = uniform tension per unit length at the boundary of the membrane.

Comparing eqn (15) and eqn (17), it is noticed that $p/T = G\theta_1$ and that the stress function Ψ corresponds to the membrane displacement ζ. In addition, eqn (16) indicates that the torsional moment M_T is equal to double the volume covered with the surface defined by Ψ.

The right-hand side of eqn (15) does not contain the factor of 2 which appears in the usual Saint-Venant torsion theory. This lack of the factor of 2, in conjunction with the torsional moment result of eqn (16) and with the membrane analogy of eqn (17), will deliver eqn (18) for a sufficiently slender section ($t \ll b$) with length b and width t:

$$M_T = \tfrac{1}{6}G\theta_1 bt^3 = \tfrac{1}{2}GJ_T\theta_1, \tag{18}$$

where $J_T = \Sigma\tfrac{1}{3}bt^3$ is the Saint-Venant torsion constant.

Since $M_T = GJ_T\theta_1$ (Timoshenko and Goodier, 1970) for elastic problems, the equivalent shear modulus G_p for plastic problems is reduced to half of the elastic shear modulus. Thus,

$$G_p = \tfrac{1}{2}G. \tag{19}$$

In the case of a strain hardening problem, it can be assumed that the yield locus maintains the geometric similarity and that the plastic deformation is generated by planar slip in the plane and in the direction of maximum shear stress as in the case of the yield plateau problem. Even in this case, the plane of maximum shear stress and the slip deformation can be explained by Figs 1 and 2. The difference from the yield plateau problem is that the increment of axial strain is accompanied by the increment of compressive axial stress, again corresponding to Shanley's idea. Thus, the results for the yield plateau problem can be applied to the strain hardening problem and the shear modulus is given by eqn (19).

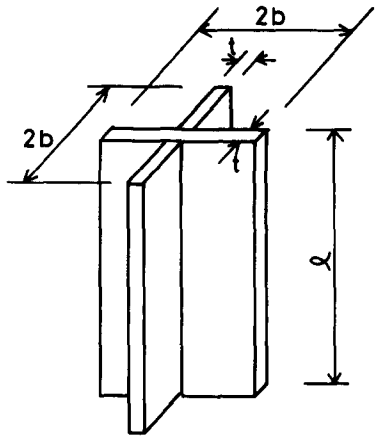

Fig. 4. Cruciform-section column.

5. BENDING STRAINS AND MOMENTS CAUSED BY BUCKLING

Figure 4 shows a cruciform section column, from which a plate element is selected as shown in Fig. 5. The plate has a free edge at $y = b$, and the other three edges are simply supported. When the plate is fully yielded in the yield plateau range under uniaxial compression, we investigate the increments of strains caused by double curvature pure bending at the instant of buckling. The flexural deformation must satisfy the following tow conditions: (1) Axial strains and flexural strains are generated without any strain reversal simultaneously in the x and y directions according to tangent modulus theory, because a lower bound for bifurcation load is sought; and (2) increments of shear strains are zero.

From condition (1), the center plane of the plate coincides with the neutral plane, and increments of strains are due only to axial strains. Therefore, eqns (4) are applicable. On the assumption that both the plane whose normal is originally in the x direction, and the plane whose normal is originally in the y direction, individually remain planar under the deformation, the strain increments at the instant of buckling are given by the following vector expression:

$$\mathrm{d}\varepsilon^{\mathrm{p}} = \mathrm{d}\varepsilon^{\mathrm{p}}_m + z\phi \quad \text{for} \quad -\frac{t}{2} \leqslant z \leqslant \frac{t}{2}, \tag{20}$$

where

$$\mathrm{d}\varepsilon^{\mathrm{p}} = \begin{pmatrix} \mathrm{d}\varepsilon^{\mathrm{p}}_x \\ \mathrm{d}\varepsilon^{\mathrm{p}}_y \end{pmatrix} = \text{incremental plastic strain vector,}$$

$$\mathrm{d}\varepsilon^{\mathrm{p}}_m = \begin{pmatrix} \mathrm{d}\varepsilon^{\mathrm{p}}_{xm} \\ \mathrm{d}\varepsilon^{\mathrm{p}}_{ym} \end{pmatrix} = \text{incremental plastic strain vector at the center of plate thickness,}$$

$$\phi = \begin{pmatrix} \phi_x \\ \phi_y \end{pmatrix} = \text{curvature vector,}$$

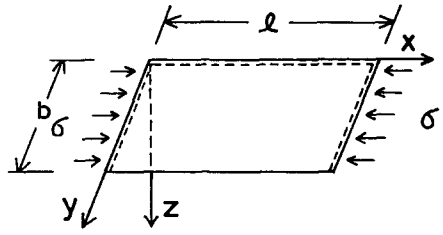

Fig. 5. One plate taken out from cruciform-section column.

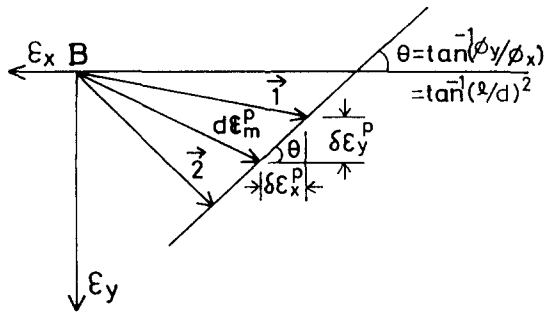

Fig. 6. Strain increment vectors at buckling.

ϕ_x = curvature in the x direction,

ϕ_y = curvature in the y direction,

z = axis along the plate thickness with an origin at the center of plate thickness,

t = plate thickness.

From eqn (20), we obtain

$$\frac{d\varepsilon_y^p - d\varepsilon_{ym}^p}{d\varepsilon_x^p - d\varepsilon_{xm}^p} = \frac{\delta\varepsilon_y^p}{\delta\varepsilon_x^p} = \frac{\phi_y}{\phi_x}, \tag{21}$$

where

$\delta\varepsilon_y^p = d\varepsilon_y^p - d\varepsilon_{ym}^p$ = plastic strain due to bending in the y direction,

$\delta\varepsilon_x^p = d\varepsilon_x^p - d\varepsilon_{xm}^p$ = plastic strain due to bending in the x direction.

Figure 6 shows the incremental plastic strain vectors at point B at the instant of buckling of a plate stressed in the yield plateau range. In this figure, $d\varepsilon_m^p$ is the incremental plastic strain vector at the center of plate thickness, and $\vec{1}$ and $\vec{2}$ are the incremental plastic strain vectors in the outer and inner fibers, respectively. The ends of these vectors lie on a single line.

Figure 7 shows the Tresca yield criterion, in which point B indicates the yielding under uniaxial compression. Assuming that buckling takes place at point B, incremental strain vectors $\vec{1}$ and $\vec{2}$ defined in Fig. 6 are shown on the Tresca yield locus. When vectors $\vec{1}$ and $\vec{2}$ at any location in the plate are inside of the angle $\angle ABC$, flexural deformation is generated by the plastic strain increments without any strain reversal. Furthermore, the stress in the plate section remains $-\sigma_0$, and the bending moments per unit width about the y- and x-axes, represented by M_x and M_y, respectively, are equal to zero. The necessary condition for vectors $\vec{1}$ and $\vec{2}$ to be inside of the angle $\angle ABC$ will be derived in Chapter 7, where it is proved that there exists a deformation satisfying conditions (1) and (2).

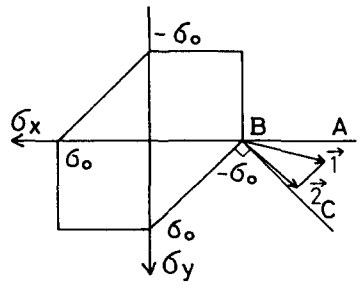

Fig. 7. Strain increment vectors and yield locus.

For plate buckling in the strain hardening range, the strains consist of elastic components as well as plastic ones. Now however M_x is not zero, because the axial compression is elevated due to strain hardening. The above discussion can be applied to the plastic components of the strains and the plate buckling in the strain hardening range will be treated in the Appendix.

6. PLASTIC BUCKLING OF STEEL PLATES IN A CRUCIFORM-SECTION COLUMN

In this chapter, we examine the buckling behavior in the yield plateau range of a single plate extracted from a cruciform-section column under uniaxial compression shown in Fig. 5. The relations between bending moments and stiffnesses, and between torsional moment and stiffness for an orthotropic plate are given by (Girkmann, 1956)

$$\left.\begin{aligned} M_x &= D_x I\phi_x + D_{xy} I\phi_y \\ M_y &= D_y I\phi_y + D_{yx} I\phi_x \\ M_{xy} &= 2G_p I\phi_{xy} \end{aligned}\right\}, \tag{22}$$

where

M_{xy} = torsional moment per unit width of the plate,

$D_x I$, $D_y I$, $D_{xy} I$, $D_{yx} I$ = bending stiffnesses,

$$I = \frac{t^3}{12},$$

ϕ_{xy} = twist of the surface with respect to the x- and y-axes.

In the previous chapter, it was shown that $M_x = M_y = 0$, or $D_x = D_y = D_{xy} = D_{yx} = 0$, and $G_p = \frac{1}{2}G$ when buckling occurs in the yield plateau range.

The equilibrium equation for plate buckling is given by

$$\frac{\partial^2 M_x}{\partial x^2} - 2\frac{\partial^2 M_{xy}}{\partial x\,\partial y} + \frac{\partial^2 M_y}{\partial y^2} = N\frac{\partial^2 w}{\partial x^2}, \tag{23}$$

where

$N = \sigma_{cr} t$ = bifurcation strength per unit width (positive for compression),

σ_{cr} = bifurcation stress,

w = out-of-plane displacement of the plate.

Substituting $\phi_{xy} = (\partial^2 w/\partial x\,\partial y)$ into the third equation of eqns (22), we obtain

$$M_{xy} = 2G_p I\frac{\partial^2 w}{\partial x\,\partial y} = GI\frac{\partial^2 w}{\partial x\,\partial y}. \tag{24}$$

Substituting the relations of $M_x = M_y = 0$ and eqn (24) into eqn (23), we obtain

$$\frac{\partial^4 w}{\partial x^2\,\partial y^2} + \frac{N}{2GI}\frac{\partial^2 w}{\partial x^2} = 0. \tag{25}$$

The out-of-plane displacement is assumed to be:

$$w = f(y)g(x). \tag{26}$$

Substituting eqn (26) into eqn (25), we obtain

$$\ddot{g}(x)[f''(y)+\frac{N}{2GI}f(y)]=0, \tag{27}$$

where $\dot{}$ and $'$ indicate derivatives with respect to x and y, respectively. The boundary conditions are represented by

$$\left.\begin{aligned}&g(x)=0 \quad \text{at } x=0, l,\\&f(y)=0 \quad \text{at } y=0,\\&Q_y+\frac{\partial M_{yx}}{\partial x}=0 \quad \text{at } y=b \text{ from Kirchhoff condition for a free edge,}\\&\text{where}\\&Q_y=\frac{\partial M_y}{\partial y}-\frac{\partial M_{xy}}{\partial x}=-\frac{\partial M_{xy}}{\partial x}.\end{aligned}\right\} \tag{28}$$

Equation (27) is satisfied by the following two relations: $\ddot{g}(x)=0$ and $f''(y)+(N/2GI)f(y)=0$. Considering the boundary conditions at $x=0$ and l, the former relation reduces to $g(x)=0$, or $w=0$, which is a trivial solution representing no buckling. The general solution for the latter relation is given by

$$f(y)=A\sin\sqrt{\frac{N}{2GI}}y+B\cos\sqrt{\frac{N}{2GI}}y. \tag{29}$$

From the boundary condition at $y=0$, we obtain

$$f(y)=A\sin\sqrt{\frac{N}{2GI}}y. \tag{30}$$

Thus,

$$w=A\sin\sqrt{\frac{N}{2GI}}y\cdot g(x). \tag{31}$$

From the boundary condition at $y=b$, we obtain

$$\frac{\partial M_{xy}}{\partial x}-\frac{\partial M_{yx}}{\partial x}=2\frac{\partial M_{xy}}{\partial x}=0. \tag{32}$$

From eqns (24), (31) and (32), we obtain

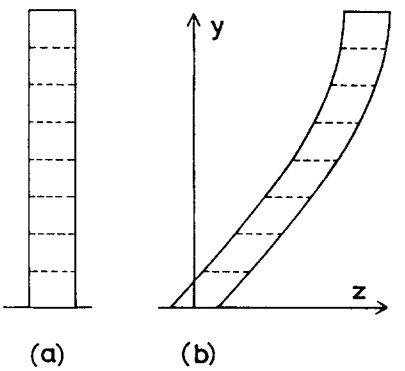

Fig. 8. Buckling mode.

$$\cos\sqrt{\frac{N}{2GI}}y\cdot\ddot{g}(x)=0. \tag{33}$$

Thus,

$$\sqrt{\frac{N}{2GI}}b=\frac{\pi}{2}. \tag{34}$$

Finally, the following bifurcation strength and stress are obtained:

$$N=\frac{\pi^2}{2b^2}GI, \tag{35}$$

$$\sigma_{cr}=\frac{\pi^2}{24}G\left(\frac{t}{b}\right)^2. \tag{36}$$

The function $g(x)$ is required only to satisfy the boundary conditions $g(0)=g(l)=0$.

7. MODE OF BUCKLING WAVE AND ASSOCIATED STRAIN AND DEFORMATION

The general solutions for the mode of buckling wave in the direction of plate width are represented by eqns (29) and (A10) for bucklings in the plastic flow range and in the strain hardening range, respectively. They must satisfy the boundary conditions given by eqns (28) which are valid both for a simply-supported edge and a fixed edge at $y=0$. Therefore, these different support conditions have the same bifurcation stress and the same mode of buckling wave (sine wave in the direction of plate width). As described in Chapter 3, shear deformation can take place at the instant of torsional buckling. Thus, the mode of buckling wave in the direction of plate width satisfying the above-mentioned boundary conditions must be accompanied by the shear deformation as shown in Fig. 8. Figure 8(a) shows the original shape and Fig. 8(b) shows the buckling mode. In these figures, the plate section is divided into sub-sections. The inner boundary lines between sub-sections in the buckling mode are parallel to the original inner boundary lines. This reflects that plastic shear angle $d\gamma_{yz}^p$ resulting from simple shear strain. Therefore, the previously *assumed* condition (3) of Chapter 3 is in fact a *necessary* condition. The increment of plastic shear strain along the plate width is maximum at the supported edge and is zero at the free edge. With respect to bending, curvature ϕ_y in the y direction for the mode shown in Fig. 8 is zero at any point in the plate. On the basis that buckling takes place with a combined mode of torsion and bending, the strain and deformation for individual modes are investigated in the following sections.

7.1. *Strain and deformation for torsional mode*

As indicated in Fig. 8, the increment of plastic shear strain $d\gamma_{yz}^p$ is maximum at the center $(l/2, 0)$ of the supported edge. Considering that the angle of the slip plane at this point is formed such that the absolute value of $d\gamma_{yz}^p$ is maximum, the maximum absolute value is obtained as $d\gamma_{yz}^p=-\lambda$ when $k=\pi/4$ from eqn (3). The out-of-plane displacement w is given by eqn (31), but $g(x)$ involved in this equation is indeterminate in the yield flow range. In the strain hardening range, however, $g(x)$ is given by eqn (A7), and thus the mode of buckling in the yield flow range satisfying the equilibrium equation is assumed as follows for the time being from modifying eqn (A12):

$$w=Q\sin\frac{\pi}{2b}y\cdot\sin\frac{\pi}{l}x. \tag{37}$$

Deriving eqn (37), $\sqrt{H}$ is calculated from eqn (A14), and m is unity in order to minimize the bifurcation strength. From Fig. 8 and eqn (37), $d\gamma_{yz}^p$ is given by

$$\mathrm{d}\gamma_{yz}^{\mathrm{p}} = \frac{\partial w}{\partial y} = \frac{\pi}{2b} Q \cos\frac{\pi}{2b} y \cdot \sin\frac{\pi}{l} x. \tag{38}$$

Since $\mathrm{d}\gamma_{yz}^{\mathrm{p}} = -\lambda$ at point $(l/2, 0)$, we obtain

$$\lambda = -\frac{\pi}{2b} Q. \tag{39}$$

From eqns (3) and (39), we have the relation

$$-\lambda \sin 2k = \frac{\pi}{2b} Q \sin 2k. \tag{40}$$

Equations (3), (38) and (40) give

$$\sin 2k = \cos\frac{\pi}{2b} y \cdot \sin\frac{\pi}{l} x. \tag{41}$$

Therefore, we find the following expression:

$$k = \tfrac{1}{2} \sin^{-1}\left(\cos\frac{\pi}{2b} y \cdot \sin\frac{\pi}{l} x\right). \tag{42}$$

It is noticed from eqn (3) that the same amount of $\mathrm{d}\gamma_{yz}^{\mathrm{p}}$ is generated for $k' = \pi/2 - k$ and that the complex slip planes defined by k and k' are possible.

7.2. *Strain and deformation for bending mode*

The curvature in the y direction denoted by ϕ_y is zero when the buckling mode shown in Fig. 8(b) takes place. Considering that the increment of plastic shear strain is generated only in the yz-plane, the curvature in the x direction denoted by ϕ_x is represented by the following equation upon using w as given by eqn (37):

$$\phi_x = -\frac{\partial^2 w}{\partial x^2} = Q\left(\frac{\pi}{l}\right)^2 \sin\frac{\pi}{2b} y \cdot \sin\frac{\pi}{l} x. \tag{43}$$

The value of ϕ_x takes the following maximum at point $(l/2, b)$:

$$\phi_{x,\max} = \left(\frac{\pi}{l}\right)^2 Q. \tag{44}$$

In Fig. 6, which shows the general expression of $\phi_y \neq 0$, vectors $\vec{1}(l/2, b, -t/2)$ and $\vec{2}(l/2, b, t/2)$ are found to make a maximum angle in the plate. Since $\phi_y/\phi_x = 0$ at any point in the plate, ends of the incremental plastic strain vectors lie on a single line.

Next, we investigate the condition that vectors $\vec{1}(l/2, b, -t/2)$ and $\vec{2}(l/2, b, t/2)$ remain in the angle $\angle ABC$ in Fig. 7. Since the incremental strain vector $\mathrm{d}\varepsilon_m^{\mathrm{p}}$ at the center of plate

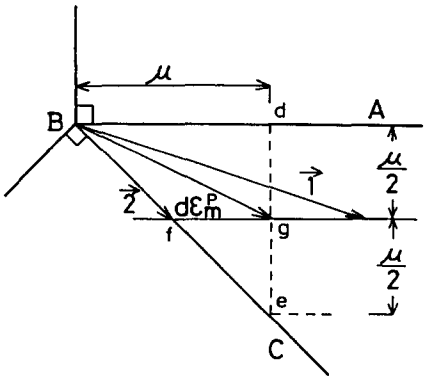

Fig. 9. Strain increment vectors at limit state.

thickness shown in Fig. 9 consists only of axial strains, its components are represented by $(-\mu, \mu/2)$ as shown by eqn (4). Since the triangle ΔBde is an equilateral right-angled triangle, $ge = \mu/2$ and $fg = \mu/2$. Considering that the maximum value of the flexural strain component in the x direction of vector $\vec{2}$ is $t/2\phi_{x,\max}$, the limit condition that vector $\vec{2}$ lies just on line BC is given by

$$\frac{t}{2}\phi_{x,\max} \leqslant \frac{\mu}{2}. \tag{45a}$$

The condition that vector $\vec{1}$ does not lie out of line BA is automatically satisfied by eqn (45). Thus, eqn (45) can be rewritten as follows when only the sign of equality is taken into account:

$$\left(\frac{\pi}{l}\right)^2 Qt = \mu. \tag{45b}$$

Equation (45b) represents the limit condition that the axial strain and the flexural strain are simultaneously developed both in the x and y directions at the instant of buckling without any strain reversal.

Next, we investigate the possible combinations of slip components resulting from flexural deformation in the plate under the limit state of no strain reversal represented by conditions (1) and (2) in Chapter 5. Substituting eqns (4), which represent the axial strain increments at the center of plate thickness, and eqn (45b) into eqn (20), we obtain

$$\begin{aligned} \mathrm{d}\varepsilon_x^{\mathrm{p}} &= -\left(\frac{\pi}{l}\right)^2 Qt + z\phi_x, \\ \mathrm{d}\varepsilon_y^{\mathrm{p}} &= \frac{1}{2}\left(\frac{\pi}{l}\right)^2 Qt. \end{aligned} \tag{46}$$

From eqns (3) and (46), the increment of plastic strain in the x direction is given by

$$\lambda = -\,\mathrm{d}\varepsilon_x^{\mathrm{p}} = \left(\frac{\pi}{l}\right)^2 Qt - z\phi_x. \tag{47}$$

In order to satisfy the condition that the increment of shear strain must be zero, we obtain $k = 0$ or $\pi/2$ according to eqn (3). Assuming that the increment of plastic strain given by eqn (47) is represented by $\xi\lambda$ in the slip plane of $k = 0$ and by $(1-\xi)\lambda$ in the slip plane of $k = \pi/2$, the increment of plastic strain in the y direction is given by

$$d\varepsilon_y^p = \xi\lambda\cos^2 0 + (1-\xi)\lambda\cos^2\frac{\pi}{2} = \xi\lambda. \tag{48}$$

From $d\varepsilon_y^p$ in eqn (46) and λ in eqn (47), ξ is represented by

$$\xi = \frac{d\varepsilon_y^p}{\lambda} = \frac{\frac{1}{2}\left(\frac{\pi}{l}\right)^2 Qt}{\left(\frac{\pi}{l}\right)^2 Qt - z\phi_x}. \tag{49}$$

At point $(l/2, b)$, substituting eqn (44) into eqn (49), we obtain

$$\xi = \frac{t}{2(t-z)}. \tag{50}$$

Thus, the following slip ratios in the direction of plate thickness are obtained:

$$\xi_0 = \tfrac{1}{2} \quad \text{for } z = 0,$$

$$\xi_{t/2} = 1 \quad \text{for } z = \frac{t}{2},$$

$$\xi_{-t/2} = \tfrac{1}{3} \quad \text{for } z = -\frac{t}{2}.$$

The slip ratio at an arbitrary point in the plate can be obtained from eqn (49) corresponding to its coordinates (x, y, z). From the above discussion it follows that the flexural deformation satisfying conditions (1) and (2) in Chapter 5 can be developed at the instant of plate buckling. It should be noted that the stress at any point in the plate remains at the yield stress and that bending moments M_x and M_y are not generated.

8. COMPARISON WITH EXPERIMENTAL RESULTS

The elastic bifurcation stress of a plate in which three edges are simply supported and one edge is free is given by the following equation when the plate is sufficiently long (Bleich, 1952):

$$\sigma_{cr} = 0.425\frac{\pi^2 E}{12(1-\nu^2)}\left(\frac{t}{b}\right)^2. \tag{51}$$

The bifurcation stress given by eqn (51) is equal to the following bifurcation stress in pure torsion when $\nu = 0.3$:

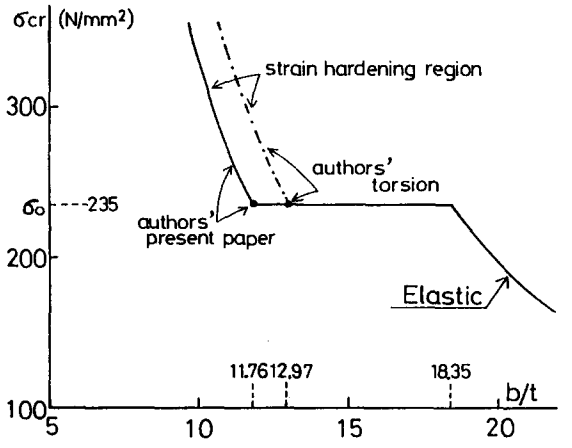

Fig. 10. Buckling curve for stress.

Table 1. Mechanical property of steel from tension test

Material	σ_Y (N mm^{-2})	σ_{max} (N mm^{-2})	ε_Y (%)	ε_{st} (%)	ε_{max} (%)	E_{st} (N mm^{-2})
SS400	265	403	0.129	2.09	17.4	3668

$$\sigma_{cr} = G\left(\frac{t}{b}\right)^2. \tag{52}$$

The bifurcation stress of a plate in torsion in the plastic range is represented by the following equation, because shear modulus G_p defined by eqn (19) is only the mechanical property related to the bifurcation stress in this case:

$$\sigma_{cr} = \tfrac{1}{2}G\left(\frac{t}{b}\right)^2. \tag{53}$$

Most of the previous research concluded that the shear modulus in the plastic flow range is equal to that in the elastic range, and that eqn (52) is valid even in the plastic flow range. The bifurcation stress in the plastic flow range given by eqn (36) obtained in this study is lower than the bifurcation stress given by eqn (53) for torsion.

The solid line in Fig. 10 shows the buckling curve calculated from eqn (36) for a mild steel designated by JIS-SS400 (yield stress $\sigma_0 = 235$ N mm^{-2}). In this figure, the curves calculated from the elastic solution eqn (52) and torsion solution eqn (53) are also illustrated as references. In Fig. 10, the intersection of the curve defined by eqn (36) and the line defined by $\sigma_x = \sigma_0$ is the only meaningful point in the plastic flow range. For the strain hardening range, eqn (A17) is applicable, which has a minimum value coincident with eqn (36) at $l/b = \infty$, which is also illustrated in Fig. 10.

In order to verify the accuracy of analysis, the following experiment was carried out. The specimens were made of mild steel plates, and the plates were assembled by welding into a cruciform section. After welding, the specimens were annealed. The plate thickness was 9 mm, the width-to-thickness ratio b/t was ranged from 5 to 15, where b indicates half of the entire width of the cruciform section, and the length $l = 3b$. The material properties obtained from a tensile test are shown in Fig. 11 and Table 1. In this table, the following symbols are used:

σ_Y = yield stress,

σ_{max} = maximum stress,

ε_Y = yield strain (σ_Y/E)

ε_{st} = strain at the onset of strain hardening,

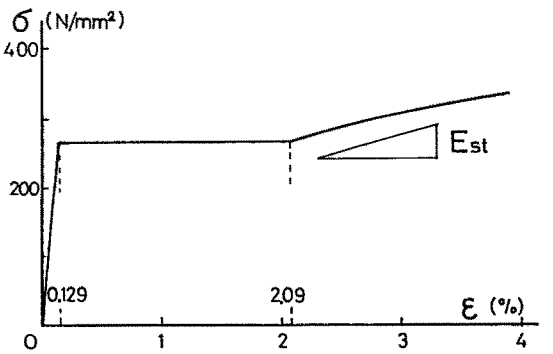

Fig. 11. Stress–strain curve.

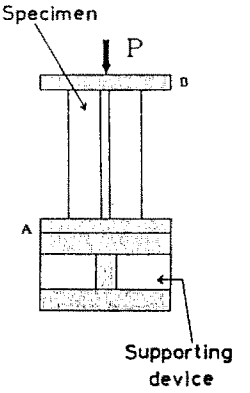

Fig. 12. Test set-up.

ε_{max} = strain at maximum stress,

E = Young's modulus,

E_{st} = strain hardening modulus.

The average yield stress obtained from the compression test, denoted by ${}_c\bar{\sigma}_Y$, was 272 N mm^{-2}, which was about 3% higher than that from the tensile test. Thus, the average yield strain in compression, denoted by ${}_c\bar{\varepsilon}_Y$, was calculated from the following equation:

$$ {}_c\bar{\varepsilon}_Y = {}_c\bar{\sigma}_Y/E. \tag{54}$$

Then, by using ${}_c\bar{\varepsilon}_Y$ obtained from eqn (54), the equivalent width-to-thickness ratio $b/t\sqrt{{}_c\bar{\varepsilon}_Y}$ was estimated.

The load was applied in a screw-type universal testing machine with a loading capacity of 2000 kN. The specimen was placed between bearing plates A and B as shown in Fig. 12. The bottom bearing plate A was set on a sufficiently stiff supporting device. The specimen was centrally loaded, and rotation was prevented.

The analytical bifurcation stress given by eqn (36) does not include the effect of length, because the plate is in the plastic flow range. The bifurcation stress in the strain hardening range given by eqn (A17) includes the effect of length. However, the difference between them is small, e.g. at most 1.4% when $l/b = 3$ and $E/E_{st} = 40$. Therefore, the buckling curve obtained from eqn (36) is compared with the test results.

Dividing both sides of eqn (36) by σ_0, we obtain a new buckling curve which is not dependent on the yield stress. Thus,

$$ \frac{\sigma_{cr}}{\sigma_0} = \frac{\pi^2}{48(1+\nu)} \cdot \frac{1}{\left(\frac{b}{t}\sqrt{{}_c\bar{\varepsilon}_Y}\right)^2}. \tag{55}$$

Assuming that the buckling stress obtained from the test is equal to σ_{max}, and substituting σ_{max} into σ_{cr} in eqn (55), we obtain

$$ \frac{\sigma_{max}}{\sigma_0} = \frac{\pi^2}{48(1+\nu)} \cdot \frac{1}{\left(\frac{b}{t}\sqrt{{}_c\bar{\varepsilon}_Y}\right)^2}. \tag{56}$$

Figure 13 shows the analytical results from eqn (56) and the experimental results, where ${}_c\bar{\sigma}_Y$ was used instead of σ_0. Equation (56) gives the stress increase rate. The solutions

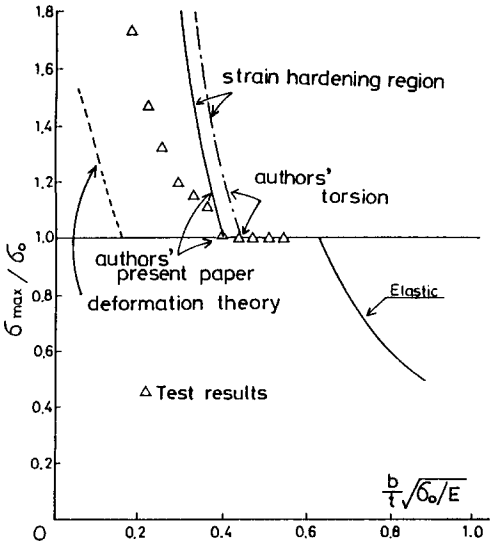

Fig. 13. Comparison of theoretical results with test results.

derived from deformation theory by Stowell (1948) on the basis of Fig. 11 and Table 1 are also shown in Fig. 13. In Fig. 13, the ordinate is the stress increase rate, and the abscissa is the equivalent width-to-thickness ratio. This figure demonstrates that the analysis and the experiment have exceptional agreement with respect to the upper limit of the width-to-thickness ratio range in which axial stress can be increased over the yield stress into the strain hardening range. With the decrease in the effective width-to-thickness ratio in the strain hardening range, the stress increase rate becomes larger, but the experimental data points are below the analytical predictions. The reason for this discrepancy is not apparent, but may be due to the loss of geometric similarity of the yield locus in the strain hardening range, which is the basic assumption in this analysis. When the geometric similarity is impaired, slip deformations in different directions can be combined. However, it can be concluded that the proposed analytical method provides a good agreement with the experimental results in the early plastic zone. This agreement results from the significant reduction in the shear modulus derived in this study.

9. SUMMARY AND CONCLUSIONS

(1) On the basis of the Tresca yield criterion and assuming that the plastic deformation is generated by planar slip in the direction of the maximum shear stress, the slip deformation in an arbitrary slip plane was represented by strains in the fixed coordinate system.

(2) When plastic buckling takes place in a single plate extracted from a cruciform-section column, a complex buckling mode composed of torsional and flexural deflections is generated, allowing us to determine an equivalent shear modulus and flexural stiffnesses in the plastic flow range. These properties were derived from the idea that plastic buckling can be developed under the combination slip obtained from (1) when there is no strain reversal.

(3) The shear modulus in the plastic flow range, and even in the strain hardening range, is equal to half of the elastic shear modulus, i.e. $1/2G$.

(4) All of the flexural stiffnesses are equal to zero in the plastic flow range, but in the strain hardening range it follows that $D_x I = E_{st} I$ while the other stiffnesses remain zero.

(5) For buckling in the plastic flow range, the buckling wave mode in the longitudinal direction must satisfy the condition that the displacement at the boundary is equal to zero, but is otherwise arbitrary. For buckling in the strain hardening range, the buckling mode in the longitudinal direction is sinusoidal. The buckling mode in the transverse direction is sinusoidal both for the plastic flow and for the strain hardening ranges.

(6) Since the boundary condition at the instant of buckling is common to the simply supported edge and the fixed edge at $y = 0$, the bifurcation stress and the buckling wave mode are also common to the different support conditions.

(7) At the instant of buckling, the increment of plastic shear strain is generated in the transverse section, and its value is maximum at the support and is zero at the free edge.

(8) Analytical solutions for the plastic buckling were compared with experimental results, and a good agreement in the early plastic zone was obtained.

REFERENCES

Batdorf, S. B. (1949). Theories of plastic buckling. *J. Aero. Sci.* **July,** 405–408.

Batdorf, S. B. and Budiansky, B. (1949). A mathematical theory of plasticity based on the concept of slip. NACA Tech. Note No. 1871.

Bleich, F. (1952). *Buckling Strength of Metal Structures.* McGraw-Hill, New York.

Budiansky, B. (1959). A reassessment of deformation theories of plasticity. *Trans. ASME 81, Series E, J. Appl. Mech.* **26,** 259–264.

Christoffersen, J. and Hutchinson, J. W. (1979). A class of phenomenological corner theories of plasticity. *J. Mech. Phys. Solids* **27,** 465–487.

Girkmann, K. (1956). *Flachentragwerke.* Springer, Berlin.

Hill, R. (1958). A general theory of uniqueness and stability in elastic–plastic solids. *J. Mech. Phys. Solids* **6,** 236–240.

Hill, R. (1966). Generalized constitutive relation for incremental deformation of metal crystals by multislip. *J. Mech. Phys. Solids* **14,** 95–102.

Hutchinson, J. W. and Budiansky, B. (1976). Analytical and numerical study of the effects of initial imperfections on the inelastic buckling of a cruciform column. Buckling of structures. Symposium, Cambridge/USA. 17–21 June, 1974, pp. 98–105. Springer, Berlin.

Inoue, T., Orihara, S. and Kuwamura, H. (1989). Stress–strain relations of cruciform section stub-columns. *J. Struct. Engng* **35B,** 323–336 (in Japanese).

Onat, E. T. and Drucker, D. C. (1953). Inelastic instability and incremental theories of plasticity. *J. Aero. Sci.* **20,** 181–186.

Ore, E. and Durban, D. (1989). Elastoplastic buckling of annular plates in pure shear. *J. Appl. Mech.* **56,** 644–651.

Prandtl (1903). Zur Torsion von prismatischen Stäben. *Physik. Z.* **4**(26b), 758–759.

Saint-Venant (1855). de Barre, Mem. acad. Sci. Savants etrangers, XIV, 233–560.

Sewell, M. J. (1973). A yield-surface corner lowers the buckling stress of an elastic–plastic plate under compression. *J. Mech. Phys. Solids* **21,** 19–45.

Sewell, M. J. (1974). A plastic flow rule at a yield vertex. *J. Mech. Phys. Solids* **22,** 469–490.

Shanley, F. R. (1947). Inelastic column theory. *J. Aero. Sci.* **14**(5), 261–267.

Stowell, E. Z. (1948). A unified theory of plastic buckling of columns and plates. NACA Technical Note, No. 1556.

Timoshenko, S. P. and Goodier, J. N. (1970). *Theory of Elasticity.* McGraw-Hill, New York.

APPENDIX: BUCKLING IN THE STRAIN HARDENING RANGE

The shear modulus in the strain hardening range is given by eqn (19) as discussed in Chapter 4. In this appendix, the flexural stiffnesses are investigated.

It is assumed that the Tresca yield locus is proportionally expanded in the strain hardening range, and that the plastic deformation is attributed to the slip deformation in the plane and in the direction of maximum shear stress in the same manner as used for the plastic flow range. The plastic components in the increments of normal strains for the strain hardening range follow the same rule discussed for the plastic flow range. The relationships between increments of strain and stress are related to the increments of shear strain caused by slip and shear stress. In the case of pure flexural deformation, the direction of the slip must be represented by $k = 0$ and $\pi/2$ as described in the case of the plastic flow range. The increments of shear strains caused by slips can be transformed into the fixed coordinate system in a one–one relation, and eqn (3) can be applied both to the cases of $k = 0$ and $\pi/2$.

The increment of shear stress related to the slip in the direction of $k = 0$ results in the stress increments of compression in the x direction and tension in the y direction, but the quantitative relation between them is now indeterminate. In an exact sense, the relation must be determined such that the bifurcation load is minimum. This discussion, however, assumes that only the increment of compressive stress in the x direction is generated. The increment of shear stress related to the slip in the direction of $k = \pi/2$ results in the stress increment in the x direction, because the stress in the z direction is zero.

When the slip results only in the stress increment in the x direction, the slip is considered to be the same kind of slip observed in coupon test of material in tension. Thus, the relations between the increments of stress and strain in the x direction, and the stress increments in the y direction, both for the cases of $k = 0$ and $\pi/2$, are given by the following equations representing the tensile behavior of the material:

$$\left.\begin{aligned} \mathrm{d}\sigma_x &= E_{\mathrm{st}}\,\mathrm{d}\varepsilon_x \\ \mathrm{d}\sigma_y &= 0 \end{aligned}\right\}, \tag{A1}$$

where

$d\sigma_x$ = increment of normal stress in the x direction,

$d\sigma_y$ = increment of normal stress in the y direction,

$d\varepsilon_x$ = increment of normal strain in the x direction,

E_{st} = tangent modulus on stress–strain curve of material in the strain hardening range.

The bending moments with respect to the y and x axes are given by

$$\left.\begin{aligned} M_x &= \int_{-t/2}^{t/2} d\sigma_x z\, dz \\ M_y &= \int_{-t/2}^{t/2} d\sigma_y z\, dz \end{aligned}\right\}. \tag{A2}$$

Substituting eqn (A1) into eqn (A2), we obtain

$$\left.\begin{aligned} M_x &= E_{st} I \phi_x \\ M_y &= 0 \end{aligned}\right\}. \tag{A3}$$

Comparing eqn (A3) with eqn (22), we obtain the following flexural stiffnesses:

$$\left.\begin{aligned} D_x I &= E_{st} I \\ D_y I &= D_{xy} I = D_{yx} I = 0 \end{aligned}\right\}. \tag{A4}$$

From eqn (A4) and eqn (22) with the relation $\phi_x = -(\partial^2 w/\partial x^2)$, the bending moments and torsional moment are represented by

$$\left.\begin{aligned} M_x &= -E_{st} I \frac{\partial^2 w}{\partial x^2} \\ M_y &= 0 \\ M_{xy} &= GI \frac{\partial^2 w}{\partial x\, \partial y} \end{aligned}\right\}. \tag{A5}$$

Substituting eqns (A5) into eqn (23) representing the equilibrium at the instant of buckling, we obtain

$$E_{st} I \ddot{g}(x) f(y) + 2GI \dot{g}(x) f''(y) + N g(x) f(y) = 0. \tag{A6}$$

When the plate ends $x = 0$, l are simply supported, adding the condition $\ddot{g}(x) = 0$ at $x = 0$, l to the boundary conditions given by eqn (28) and solving eqn (A6) by the method of separation of variables, we obtain

$$g(x) = A \sin \frac{m\pi}{l} x. \tag{A7}$$

Then,

$$f''(y) + \frac{1}{2GI}\left(N - \frac{m^2\pi^2}{l^2} E_{st} I\right) f(y) = 0. \tag{A8}$$

Equation (A8) is rewritten as

$$f''(y) + Hf(y) = 0,$$

$$H = \frac{1}{2GI}\left(N - \frac{m^2\pi^2}{l^2} E_{st} I\right). \tag{A9}$$

The general solution of eqn (A9) when $H \neq 0$ is given by

$$f(y) = B \sin \sqrt{H} y + C \cos \sqrt{H} y. \tag{A10}$$

The boundary conditions are given by eqn (28). Thus, from the condition at $y = 0$

$$f(y) = B \sin \sqrt{H} y. \tag{A11}$$

Thus, the buckling mode is represented by

$$w = AB \sin \sqrt{H} y \cdot \sin \frac{m\pi}{l} x. \tag{A12}$$

From the boundary condition at $y = b$, we obtain

$$\sqrt{H}\cos\sqrt{H}y \cdot \sin\frac{m\pi}{l}x = 0. \tag{A13}$$

Thus, we obtain

$$\sqrt{H}b = \frac{\pi}{2}, \tag{A14}$$

$$N = \frac{\pi^2}{2b^2}GI + \frac{m^2\pi^2}{l^2}E_{st}I. \tag{A15}$$

N defined by eqn (A15) is minimum at $m = 1$. Thus, we obtain the following bifurcation strength and stress:

$$N = \frac{\pi^2}{2b^2}GI + \frac{\pi^2}{l^2}E_{st}I, \tag{A16}$$

$$\sigma_{cr} = \frac{\pi^2}{24}G\left(\frac{t}{b}\right)^2 + \frac{\pi^2}{12}E_{st}\left(\frac{t}{l}\right)^2$$
$$= \frac{\pi^2}{12}\left\{\frac{G}{2} + E_{st}\left(\frac{b}{l}\right)^2\right\}\left(\frac{t}{b}\right)^2. \tag{A17}$$

Assuming $H = 0$ in eqn (A9), we obtain $f(y) = Dy$ which represents a linear mode in the direction of plate width, but considering the boundary condition at $y = b$, it is noticed that this solution results in $f(y) = 0$, that is, a trivial deformation of no buckling.

Comparing eqn (A17) with eqn (36) which was derived for the plastic flow range, eqn (A17) gives a higher critical stress by the difference of the second term including E_{st} in the right-hand side of eqn (A17). However, the difference is at most 1.4% when $l/b = 3$ and $E/E_{st} = 40$.

If the distribution of the stress increment in the x and y directions does not follow the assumption that $d\sigma_y = 0$, we may obtain a smaller bifurcation stress. However, since the analysis based on this assumption provides a satisfactory agreement with the bifurcation stress in the plastic flow range, further detailed study will not be necessary.